Appl. Magn. Reson. 26, 1–XXX (2004)

Applied Magnetic Resonance

EPR Study of Spin and Charge Dynamics in Slightly Doped Poly(3-Octylthiophene)

V. I. Krinichnyi[1] and H.-K. Roth[2]

[1] Institute of Problems of Chemical Physics, Russian Academy of Sciences, Chernogolovka, Russian Federation
[2] Department of Physical Materials Research, TITK Institute Rudolstadt, Rudolstadt, Germany

Received June 2, 2003; revised November 27, 2003

Abstract. An initial virgin plasticine-like poly(3-octylthiophene) (P3OT) and this sample modified by annealing and recrystallization were investigated mainly at X-band (10 GHz) and at D-band (140 GHz) electron paramagnetic resonance (EPR) in a wide temperature region. Paramagnetic centers with anisotropic magnetic-resonance parameters were proved to exist in all polymers, namely, mobile polarons whose concentration and susceptibility depend on the temperature and the polymer treatment. Superslow torsional motion of the polymer chains and layers was studied by the saturation transfer method at D-band EPR. Spin-spin and spin-lattice relaxation times were measured separately by steady-state saturation method at the same waveband EPR. Intrachain and interchain spin diffusion coefficients and conductivity due to polaron dynamics were calculated. It was shown that the charge transport in P3OT is determined by the strong spin-spin interaction and is stimulated by torsion motion of the polymer chains. The total conductivity of P3OT is determined mainly by dynamics of paramagnetic charge carriers. Magnetic, relaxation and dynamics parameters of P3OT were also shown to change during the polymer treatment.

1 Introduction

The magnetic and electronic properties of organic polymer semiconductors with extended π-conjugated system, *trans*-polyacetylene (*trans*-PA) and poly(*p*-phenylene)-like, are widely studied in the last years [1–4] owing to their potential use as active materials in molecular electronics [5–7]. Particularly, polythiophene and its derivatives, poly(3-alkylthiophene) (P3AT) (Fig. 1a) have been the subject of many investigations [8, 9] as a model system for understanding the electronic and optical properties of sulphur-based one-dimensional (1-D) systems with nondegenerate ground states [8–10]. In their undoped state these organic materials are semiconductors, whose energy mid-gap is determined by the presence of the π-orbital conjugation along the main polymer axis. For P3AT the gap amounts ca 2 eV at ambient temperatures giving rise to its characteristic red color. This parameter, however, is found for P3AT [11, 12] to be temperature-dependent, so

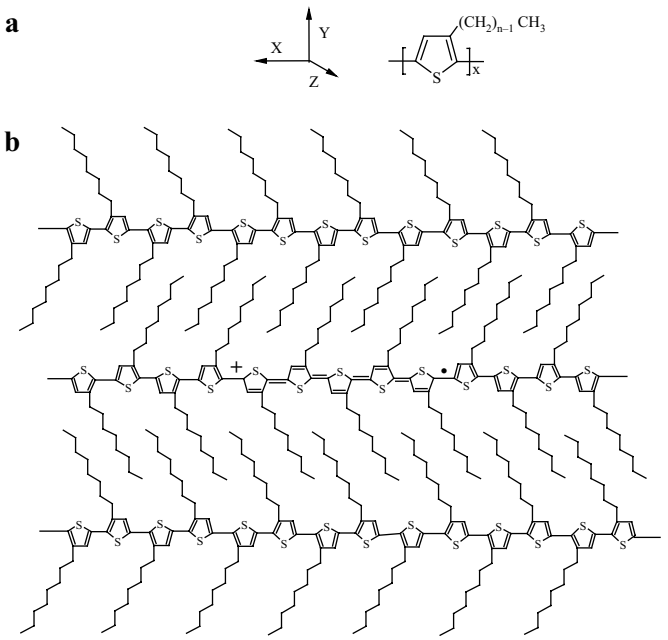

Fig. 1. Schematic structure of P3AT (**a**) and P3OT (**b**). The formation of the polaron carrying along the P3OT chain and possessing a spin $S = 1/2$ and an elemental charge e is shown.

that the color of the polymer is changed to yellow at the temperature change ('thermochromism').

For poly(3-octylthiophene) (P3OT, $n = 8$ in Fig. 1a) (Fig. 1b) the transition temperature is close to 450 K. A decrease of the optical gap was observed [13] in P3OT due to the decrease of the torsion angle between the adjacent thiophene rings and the enhancement of interchain interactions between parallel polymer planes. It is well known that the transport properties of this class of materials are mainly governed by the presence of mobile polarons originating from the synthesis and the adsorption of oxygen from ambient atmosphere (Fig. 1b) [14, 15]. This leads to an appearance in the polymer of positively charged polarons (spontaneous *p*-type doping) possessing an elemental charge e and an unpaired electron. These charge carriers are subsequently partly trapped by the impurities, as opposed to inorganic semiconductors where, in the case of *p*-type doping, the hole is transferred from the impurity to the valence band. The presence of polaron in polythiophene and its derivatives was revealed by optical absorption measurements and electron paramagnetic resonance (EPR) [16]. When the concentration y of dopant (oxygen, iodine, etc.) increases, the number of polarons increases and, starting from some doping level, the polarons combine to form diamagnetic bipolarons. P3OT is also expected to be a suitable and perspective polymer for molecular electronics [5–7, 17–19], e.g., polymer sensors [20] and polymer-fullerene solar cells [21–25]. The piezoelectric effect has been also regis-

tered in P3OT [26]. DC (direct current) conductivity of an as synthesized P3OT is about 10^{-6} Scm^{-1} [27]. McCullough et al. [28] have reported the maximum room temperature (RT) dc electrical conductivity (σ_{ac}) of I_2-doped P3AT to be 60 Scm^{-1} for poly(3-hexylthiophene) (P3HT, $n = 6$ in Fig. 1a), 200 Scm^{-1} for P3OT, 1000 Scm^{-1} for poly(3-dodecylthiophene) (P3DDT, $n = 12$ in Fig. 1a). This shows the correlation of the P3AT dc conductivity with the alkyl group length and the morphology of the sample. Kunugi et al. [29] have shown by the electrochemical study of charge transport that the RT carrier mobility in a regioregular P3OT film is $5 \cdot 10^{-3}$ $cm^2V^{-1}s^{-1}$ at $y = 1.4 \cdot 10^{-4}$. This value decreases down to $5 \cdot 10^{-4}$ $cm^2V^{-1}s^{-1}$ at $y = 1.0 \cdot 10^{-2}$ due to the scattering of polarons by ionized dopants and the formation of immobile π-dimers. Then it increases up to 0.5 $cm^2V^{-1}s^{-1}$ at $y = 0.23$ due to the formation of bipolarons, followed by the evolution of the metallike conduction. The energy levels associated with the bipolarons are empty and are located closer to the center of the gap than those associated with the polarons [30].

Polaron possesses a spin $S = 1/2$, therefore P3OT is widely studied by different magnetic resonance methods. ^1H nuclear magnetic resonance (NMR) proton spin-lattice relaxation time study of an initial and ClO_4-doped P3OT samples have shown [31] that the motion of the chain ends and the entire motion of the octyl groups occurs at different temperatures. At 3-cm waveband ($\nu = 10$ GHz, X-band) EPR of polaron in polythiophene and its derivatives is characterized by a single line with the peak-to-peak width of 6–8 G and the *g*-factor close to the *g*-factor of a free electron [16]. In the study of C_{60}-doped poly(3-octadecylthiophene) [32], P3OT [33], and P3DDT [34] at this waveband two EPR signals with different magnetic parameters attributed to the positive polaron P^+ in the polymer chains and to the C_{60}^- anion have been registered.

However, the study of organic solids with paramagnetic centers (PC) at $\nu \leqslant 10$ GHz demonstrates low spectral resolution and stronger spin exchange. These factors limit significantly the accuracy of the method and can lead to an ambiguous interpretation of the results obtained. This also is a reason that there are only a few studies of relaxation, molecular and electronic dynamic properties of P3AT.

Earlierly we have demonstrated [35–38] the advantages of the 2-mm waveband ($\nu = 140$ GHz, D-band) EPR spectroscopy in the study of spin dynamics in various polymer semiconductors, P3OT among them [39]. This paper reports first detailed results of the investigation of polaron dynamics in the initial and treated P3OT samples at X- and D-bands EPR. Some results on P3OT have been briefly reported previously [39].

2 Experimental

In the study was used regioregular Aldrich P3OT with the average molecular weight M_w ca 142000 characterized by the lattice constants of $a = 2.030$ nm, $b = 0.480$ nm, $c = 0.785$ nm [40]. One part of the initial P3OT (P3OT-I) was slowly (nearly for 1 h) heated at argon atmosphere from 300 up to 450 K, the

sample was annealed at this temperature for 2 h and then the temperature was slowly, for 2 h, decreased down to 300 K. This sample is named P3OT-A. Another part of the initial sample was firstly solved in chloroform at 300 K and then resolved and recrystallized for 2.5 h. At the next stage this sample was also annealed analogous to the P3OT-A sample. This sample is named P3OT-R.

EPR experiments were performed mainly on a D-band EPR-05 [41] and an X-band PS-100X spectrometers, with 100 kHz field modulation for phase-lock detection. The X- and D-band EPR spectra of the samples were registered in the temperature region of 90–340 K at nitrogen atmosphere. The RT total spin concentration in the samples was determined with a $Cu_2S0_4 \cdot 5H_2O$ single-crystal standard, whereas Mn^{2+} with $g_{eff} = 2.00102$ and $a = 87.4$ G was used for the determination of the g-factor as well as for the magnetic field sweep scale calibration at the D-band EPR. The total paramagnetic susceptibility of PC in the samples was determined by double integration of their EPR spectra. EPR spectra were simulated with the Microcal Origin V.7.0552 and Bruker WinEPR SimFonia V.1.25 programs.

Spin-lattice and spin-spin relaxation times of the initial and treated P3OT samples were measured separately at D-band EPR by the steady-state continuous-wave saturation method described in detail earlier [36, 42].

3 Results and Discussion

3.1 Magnetic Resonance Parameters of Polarons in P3OT

Figure 2 shows X- and D-band EPR spectra of the initial and treated P3OT samples. At the X-band the samples show a single nearly Lorentzian EPR line with $g_{eff} = 2.0019$. The asymmetry factor of the lines, i.e., the ratio of their negative amplitude (A) to the positive one (B) is $A/B \cong 1.1$, and their peak-to-peak linewidth was measured to be $\Delta B_{pp} = 2.7$ G (P3OT), 2.7 G (P3OT-A), and 2.6 G (P3OT-R) (Fig. 2a). The ΔB_{pp} value is smaller than $\Delta B_{pp} \approx 6$–8 G obtained for polythiophene and poly(methylthiophene) [16], however, is close to 3.2 G registered for polarons in regioregular P3OT [33]. The X-band EPR spectrum of the P3OT-I sample stored for two years is also shown in Fig. 2a by the dotted line. Its computer modeling has shown that it consists of anisotropic and isotropic spectra. The effective g-factors of these spectra are close; therefore one can conclude that localized paramagnetic centers with more anisotropic magnetic parameters appear during the polymer storage.

The RT total spin concentration of P3OT increases during the polymer treating from $4.1 \cdot 10^{19}$ spin/g in P3OT-I up to $3.3 \cdot 10^{20}$ spin/g in P3OT-A and $3.5 \cdot 10^{20}$ spin/g in P3OT-R or from 0.013 to 0.11 and to 0.11 spin per monomer unit, respectively. Their inverse effective paramagnetic susceptibility χ^{-1} and the χT value are presented in Fig. 3 as function of temperature. In the high-temperature region the spin susceptibility of the P3OT-I and P3OT-R samples seems to include a contribution due to a strong spin-spin interaction (Fig. 3) as it was re-

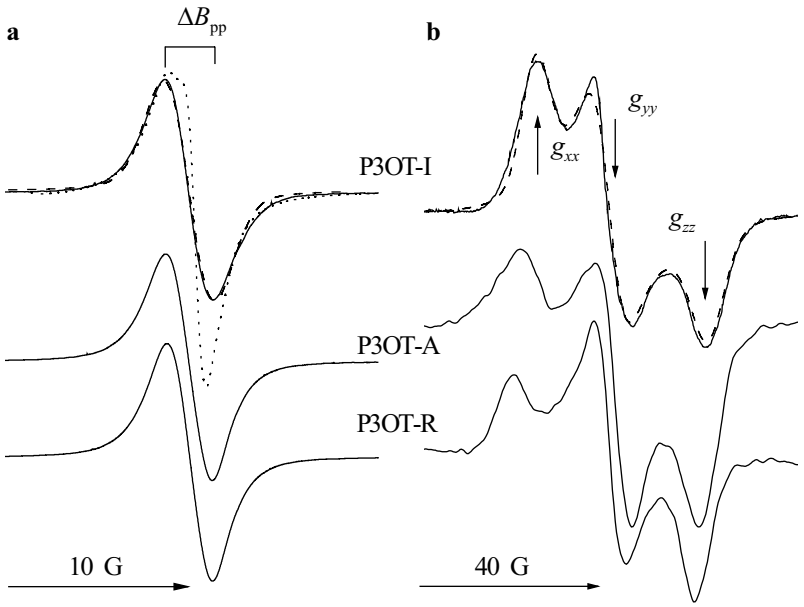

Fig. 2. RT X-band (**a**) and D-band (**b**) absorption EPR spectra of the P3OT-I, P3OT-A and P3OT-R. The X-band EPR spectrum of the P3OT-I stored for two years is shown by the dotted line. The spectra calculated with $g_{xx} = 2.004089$, $g_{yy} = 2.003322$, $g_{zz} = 2.002322$, $\Delta B_{pp}^{X} = \Delta B_{pp}^{Y} = \Delta B_{pp}^{Z} = 2.5$ G, and Lorentgian-Gaussian line shape ratio = 0.9 (**a**), and $\Delta B_{pp}^{X} = 8.2$ G, $\Delta B_{pp}^{Y} = 7.8$ G, $\Delta B_{pp}^{Z} = 8.8$ G and Lorentgian-Gaussian lineshape ratio = 0.4 (**b**) are shown by the dashed lines. The sum spectrum of the lines calculated with $g_{\|} = 2.00387$, $g_{\perp} = 2.00275$, $\Delta B_{pp} = 1.1$ G and $g_{iso} = 2.00312$ and $\Delta B_{pp} = 3.5$ G with the amplitude ratio of 2.5:1 is shown by the dotted line on the top left as well.

vealed in polyanilines [38, 43], poly(*bis*-alkylthioacetylene) [44] and poly(3-dodecylthiophenes) [45–48]. This contribution disappears at low temperatures due to the phase transition opening an energy gap at the Fermi level [16], so then the susceptibility demonstrates the Curie-Weiss behavior. In this case the total spin susceptibility follows the equation [49, 50]

$$\chi(T) = \chi_0 + \frac{C}{T-\theta} + \frac{k_1}{T}\left[\frac{\exp(-J/k_B T)}{1+3\exp(-J/k_B T)}\right]^2, \quad (1)$$

where χ_0 and k_1 are constants, C is the Curie constant, θ is the Weiss constant, k_B is the Boltzmann constant, and J is the spin-spin interaction energy.

Figure 3 shows that the $\chi(T)$ dependences are fitted well by Eq. (1) for all P3OT samples. As in the case of sulfonated polyaniline [51], these results evidence that the annealing of the P3OT polymer affects an effective exchange coupling between spins which results in the change of an effective number of the Bohr magnetons μ_B per monomer unit, however, the recrystallization neglects this effect.

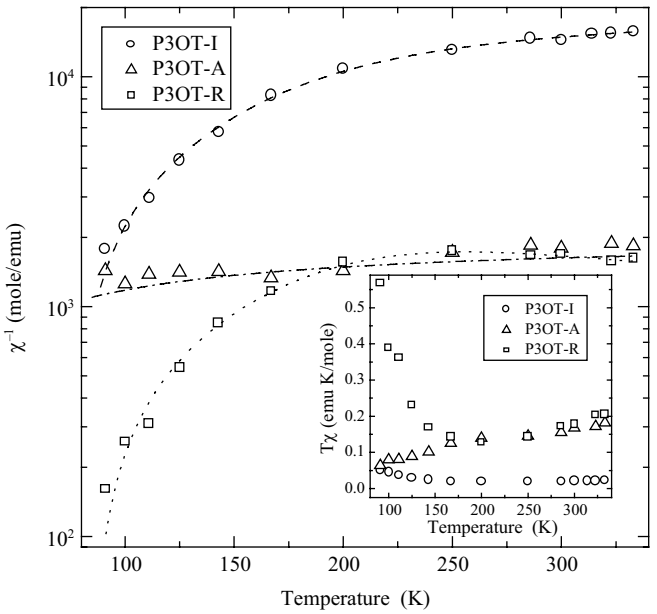

Fig. 3. Inverse $\chi(T)^{-1}$ and $T\chi(T)$ (inset) dependences of initial and treated P3OT samples. The dependences calculated from Eq. (1) with $\chi_0 = 0$, $C = 0.72 \pm 0.02$ emuK/mole, $\theta = 55.1$ K, $k_1 = 10.6$ emuK/mole, and $J = 0.0062$ eV (dashed line), $\chi_0 = 4.5 \cdot 10^{-4}$ emu/mole, $C = 0.044$ emuK/mole, $\theta = k_1 = 0$ (dotted line), $\chi_0 = 0$, $C = 4.1$ emuK/mole, $\theta = 155.6$ K, $k_1 = 52.1$ emuK/mole, and $J = 0.011$ eV (dash-dotted line) are shown as well. The error of the determination of C, θ, k_1, and J values is ± 0.02 emuK/mole, 0.2 K, ± 0.3 emuK/mole, and ± 0.4 meV, respectively.

At the D-band EPR the samples demonstrate the superposition of more broadened convoluted Gaussian and Lorentzian lines (with the Lorentgian-Gaussian lineshape ratio ca 0.4) with the anisotropic g-factor (Fig. 2b) as it is typical for PC in some other conducting polymers with heteroatoms [35, 36]. In order to determine the main magnetic resonance parameters of the samples their D- and X-band EPR spectra were compared with computed ones as it is seen in Fig. 2. From the RT spectra of P3OT-I the main components of its g-tensor have been determined to be $g_{xx} = 2.00409$, $g_{yy} = 2.00332$, $g_{zz} = 2.00235$. The treatment of the samples leads to the change of these parameters to $g_{xx} = 2.00404$, $g_{yy} = 2.00315$, $g_{zz} = 2.00231$ for P3OT-A and to $g_{xx} = 2.00402$, $g_{yy} = 2.00313$, $g_{zz} = 2.00234$ for P3OT-R. The temperature should affect the distribution of an unpaired electron in polaron changing the principal values of the g-tensor and hyperfine structure of the PC in the samples. Figures 4 and 5 show the temperature dependences of g_{xx} and g_{yy} values and the peak-to-peak linewidth ΔB_{pp} of all spectral components of the initial and treated P3OT samples determined from their spectral simulation.

The effective g-factor $g_{eff} = 1/3\sum_3 g_{ii}$ of the P3AT is higher than that of most hydrocarbonic conjugated polymers, therefore one can conclude that in P3AT the unpaired electron interacts with sulfur atoms. This is typical for other sulfur-con-

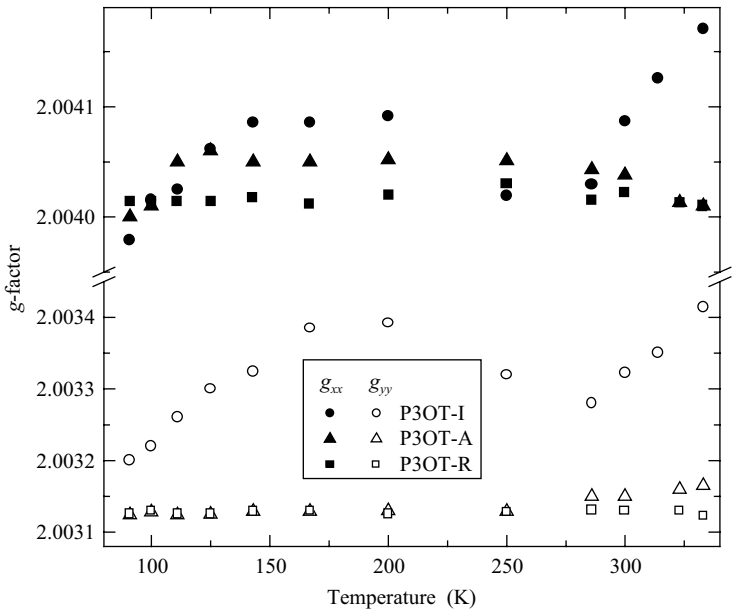

Fig. 4. Temperature dependences of the g_{xx} (closed symbols) and g_{yy} (open symbols) values determined at the X-band EPR for the P3OT-I, P3OT-A and P3OT-R. The error of the determination of the g-factor value is $\pm 3 \cdot 10^{-5}$.

taining compounds, e.g., poly(tetrathiafulvalenes) [36], poly(*bis*-alkylthioacetylene) [44] and benzo-trithioles [52] in which sulfur atoms are involved into the conjugation. The shift of the g-factor from the g_e-factor for a free electron is expressed by [53]

$$g_{ii} - g_e = g_e \lambda_s \rho_s(0) / \Delta E_{nj},$$

where $g_e = 2.00232$, $\rho_s(0)$ is the spin density on the sulfur nucleus, $\lambda_s = 0.047$ eV is the constant of the spin-orbit interaction of the electron spin with the sulfur nucleus, ΔE_{nj} is the energy of an electron excitation from the ground orbit to nearest π^* and σ^* orbits ($\Delta E_{n\pi^*}$ and $\Delta E_{n\sigma^*}$ respectively). In sulfur-based organic solids like, e.g., poly(*bis*-alkylthioacetylene) and poly(tetrathiafulvalene) in which electrons are localized mainly on the sulfur atom an effective g-factor of PC is $2.014 \leqslant g_{iso} \leqslant 2.020$ [52, 54–57]. The g-factor of PC in P3OT is much smaller so one can expect a higher spin delocalization in the monomer units. Indeed, assuming $\Delta E_{n\pi^*} \approx 2.6$ eV as typical for sulfuric solids, then the g-factor components of the initial P3OT yields the decrease in $\rho_s(0)$ by a factor of 1.8 as compared with poly(*bis*-alkylthioacetylene) [44] and by a factor of 2.6–3.9 as compared with poly(tetrathiafulvalenes) [36]. One can evaluate the lower limit of RT probability (in frequency units) for the duration of the stay of spin at the sulfur site in the P3OT samples by the total shift of the spectral components

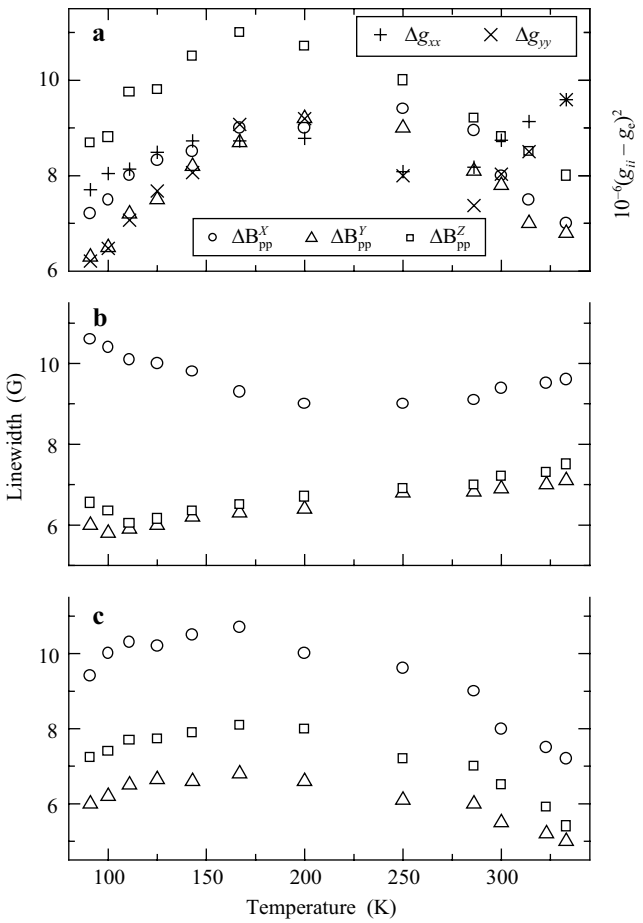

Fig. 5. Temperature dependences of the linewidth of the principal spectral components of the P3OT-I (**a**), P3OT-A (**b**) and P3OT-R (**c**) 2-mm EPR spectra. The error of the determination of the linewidth is $\pm 5 \cdot 10^{-2}$ G.

registered at the above mentioned positions g_{ii}^{P3OT} relative to the g_{ii}^{S} value typical for the sulfuric radical from the modified Heisenberg equation

$$\nu_{\mathrm{1\text{-}D}}^{0} \cong \sum_{i}^{2} (g_{ii}^{\mathrm{S}} - g_{ii}^{\mathrm{P3OT}}) \mu_{\mathrm{B}} B_0 h^{-1} \ ,$$

where B_0 is the strength of an external magnetic field and $h = 2\pi\hbar$ is the Planck constant. With g_{ii}^{P3OT} determined from the D-band EPR spectra we obtain $\nu_{\mathrm{1\text{-}D}}^{0} = 3.4 \cdot 10^{9}$ s^{-1}.

As in the case of other organic radicals, the g_{zz} values of the P3AT samples are close to the g-factor for a free electron so they feel the change in the system

properties weakly. In contrast to X-band EPR, high spectral resolution achieved at D-band EPR allows one to register separately the structure and/or dynamic changes in all spectral components. Figure 4 shows that the g_{xx} and g_{yy} values reflect the properties of the radical microenvironment more efficiently. These values of the initial P3OT decrease with the temperature decrease from 333 down to 280 K possibly due to the transition to the more planar conformation of the polymer chains. Below 280 K, these values increase at the sample freezing down to 160–220 K and then also decrease at the further temperature decrease. The decrease of g_{xx} and g_{yy} values at low temperatures can be explain by a harmonic vibration of macromolecules which evokes the crystal field modulation and is characterized by the $g(T) \propto T$ dependence [58]. After the polymer treatment, temperature weakly affects these parameters. This fact can be interpreted by the growth of the system crystallinity due to the higher chain packing in the treated polymers.

The linewidth of the spectra increases by a factor of ca 3 at the increase of the registration frequency from 10 up to 140 GHz (Fig. 5). It is seen that the linewidths of the PC in the samples depend on the polymer treatment and temperature. The treatment leads to the decrease in the averaged linewidth $\Delta B_{\mathrm{pp}} = 1/3\sum_3 \Delta B$ from 8.2 G (P3OT-I) down to 7.8 G (P3OT-A) and then to 6.7 G (P3OT-R) confirming the above supposition of the growth of the system crystallinity. The linewidth of the P3OT-I increases with the temperature increase from 90 K up to the phase transition characteristic temperature $T_{\mathrm{c}} \cong 200$ K and then decreases at the further temperature growth. The analogous tendency demonstrates P3OT-R, however, its T_{c} value decreases down to ca 170 K (Fig. 5). This effect of the linewidth decrease below T_{c} was detected also in the study of doped polyaniline [37, 38] and was not registered in other conducting polymers; it can be interpreted, e.g., as the manifestation of defrosting of molecular motion and/or acceleration of relaxation processes at low temperatures. On the other hand, the ΔB^X_{pp} value of P3OT-A decreases with the temperature increase of up to $T_{\mathrm{c}} \cong 200-250$ K and starts to increase at $T \geqslant T_{\mathrm{c}}$, whereas the other spectral components are broadened linearly with the temperature growth from 100 K (Fig. 5). If one supposes that molecular dynamics and/or electron relaxation should stimulate activated broadening of the i-th line, $\Delta B^i_{\mathrm{pp}} = \Delta B^i_{\mathrm{pp}_0} \exp(E_{\mathrm{a}}/k_{\mathrm{B}}T)$, from the slopes of these dependences it is possible to determine separately the parameters of electron relaxation and molecular dynamics near the principal macromolecular axes. The preexponential factor and the energy for activation of molecular motion near the principal X, Y and Z axes in the samples are presented in the Table 1.

Table 1. The preexponential factor ΔB_{pp_0} (in Gauss) and the activation energy E_{a} (in millielectron volts) of the molecular motion near the principal axes in the initial and treated P3OT samples.

Sample	$\Delta B^X_{\mathrm{pp}_0}$	E^X_{a}	$\Delta B^Y_{\mathrm{pp}_0}$	E^Y_{a}	$\Delta B^Z_{\mathrm{pp}_0}$	E^Z_{a}
P3OT-I	11.4	3.6	11.8	4.9	14.8	4.3
P3OT-A	12.0	7.2	7.2	2.0	7.5	2.1
P3OT-R	12.8	2.4	7.8	1.9	9.1	1.8

The analysis of the data presented in Figs. 4 and 5 shows that the linewidth can also be correlated to the spin-orbit coupling in the framework of the Elliot mechanism [59] playing an important role in the charge transfer in organic ion-radical salts [54] and five-member-ring conducting polymers [16]. Indeed, $\Delta B_{pp}^{X} = 2.8 \cdot 10^6 (g_{xx} - g_e)^2$ and $\Delta B_{pp}^{Y} = 8.1 \cdot 10^6 (g_{yy} - g_e)^2$ dependences are valid for, e.g., P3OT-I at least at $T \leqslant T_c$. This means that different mechanisms can affect the individual components of the P3OT spectrum and that the scattering of charge carriers (see below) should be governed by the potential of the polymer backbone.

3.2 Spin Relaxation of Polarons in P3OT

Figure 6 demonstrates D-band dispersion spectra of P3OT registered at different temperatures without and with π/2-shift in the phase-lock detector. It is seen that

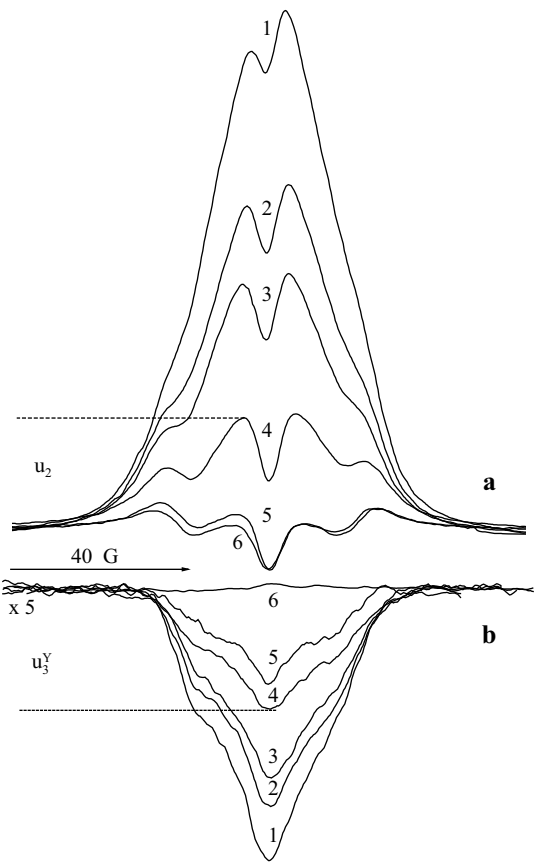

Fig. 6. In-phase (**a**) and π/2-out-of-phase (**b**) terms of the D-band dispersion EPR spectrum of the P3OT-I registered at T = 90 K (1), 100 K (2), 110 K (3), 145 K (4), 200 K (5) and 250 K (6).

in both components of the dispersion EPR signal of the P3OT the bell-like contribution with Gaussian spin packet distributions is registered. The appearance of such a component is attributed to the adiabatically fast passage of saturated spin packets by a modulating magnetic field, as discussed below.

In order to determine the influence of the polymer structure and the polymer treatment on spin and charge dynamics, the relaxation properties of all samples should be studied. Gullis [60] have shown that the first derivative of the dispersion signal U registered at adiabatically fast passage of the saturated spin-packets by a modulating magnetic field with the angular frequency ω_m generally consists of two in-phase, u_1, u_2, and one out-of-phase, u_3, terms

$$U = u_1 \sin(\omega_m t) + u_2 \sin(\omega_m t - \pi) + u_3 \sin(\omega_m t \pm \pi/2), \quad (2)$$

As for other conducting polymers [36, 42], the in-phase and π/2-out-of-phase terms of the D-band EPR dispersion signal of the samples under study contain the bell-like contribution with Gaussian spin packet distributions due to the adiabatically fast passage effect (Fig. 6). At $T \geqslant 200$ K the in-phase and π/2-out-of-phase components of the dispersion signals are determined mainly by the first and third terms of Eq. (2) (spectra 5 and 6 in Fig. 6) indicating that the inequality $\omega_m T_1 < 1$ holds for polarons in all samples. The opposite inequality is

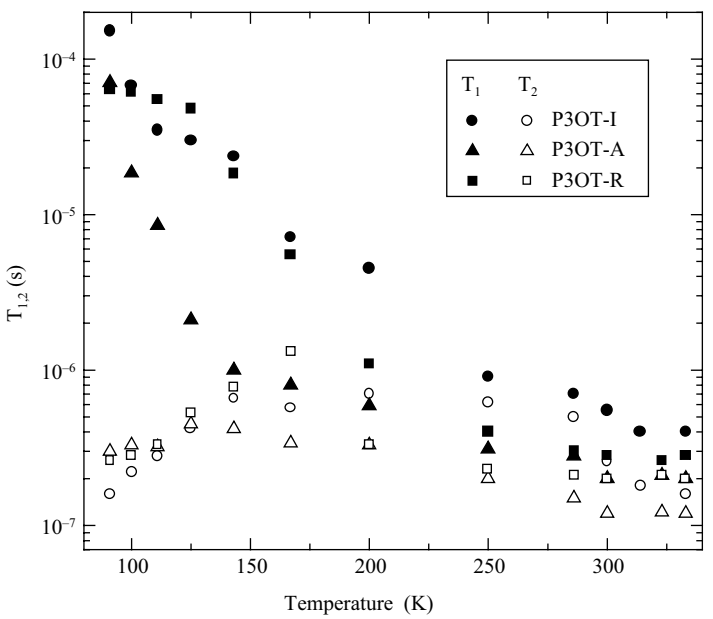

Fig. 7. Temperature dependences of the relaxation times T_1 (closed symbols) and T_2 (open symbols) of the P3OT-I, P3OT-A and P3OT-R. The error of the determination of the relaxation times does not exceed the area of the points.

fulfilled at lower temperatures when the dispersion spectrum is determined by the two last terms of Eq. (2) (spectra 1 to 4 in Fig. 6). Therefore, it is possible from the analysis of these terms to determine separately the relaxation parameters of the PC in the samples, namely, spin-lattice (T_1) and spin-spin (T_2) relaxation times.

The semilogarithmic temperature dependence of the relaxation times determined from the saturated EPR dispersion spectra according to the method described in refs. 36 and 42 are shown in Fig. 7. One can conclude from these data that the polymer treatment leads to the acceleration of the PC effective relaxation possibly due to the increase of the interaction of polaron charge carriers with the lattice phonons. As Fig. 7, the relaxation times of the samples increase simultaneously at the temperature decreases from 333 down to ca 250 K (P3OT-I, P3OT-R) and 150 K (P3OT-A). The spin-spin relaxation is accelerated below this point leading to the appropriate change of the spectral component linewidth (Fig. 6).

3.3 Macromolecular Dynamics of Chains of P3OT

It is seen from Fig. 6 that the relative intensities of the u_3 term change with the temperature. This effect evidences the appearance of the saturation transfer (ST-EPR) over the quadrature spectrum [61] due to superslow macromolecular dynamics. Earlier, it was shown [62] that from the D-band ST-EPR spectra one can estimate separately all characteristic times for the radicals with anisotropic magnetic parameters, involved in anisotropic superslow motion near different molecular axes in various solids including conducting polymers with heteroatoms [36]. In this case the correlation time of the chain segments macromolecular libration motion of the near the principal molecular, e.g., X-axis τ_c^X can be determined from the ratio of amplitudes of the $\pi/2$-out-of-phase dispersion term u_3 as

$$\tau_c^X = \tau_{c0}^X (u_3^X/u_3^Y)^{-\alpha},$$

where α is a constant determining by an anisotropy of g-factor.

The τ_c^X value determined from the $\pi/2$-out-of-phase dispersion spectra of polarons in the initial and treated P3OT samples are presented in Fig. 8 as the function of temperature. This value of P3OT-I and P3OT-A decreases with the temperature increase of up to $T_c \cong 150$ K and increases above this critical temperature (Fig. 8). The opposite temperature dependence is characteristic for $\tau_c^X(T)$ of P3OT-R with the close T_c value. Note that Masubuchi et al. [31] have observed ^{1}H NMR T_1 temperature dependence with the same critical temperature that was attributed to the defrosting of molecular motion of methyl, ethyl or propyl chain end groups. The dependences obtained can be interpreted in the frames of the superslow activation 1-D libration of the polymer chains together with polarons at low temperatures when $T \leqslant T_c$, whereas their high-temperature part can be explained by the defrosting of the collective 2-D motion at $T \geqslant T_c$. In this case an the effective correlation time is determined as

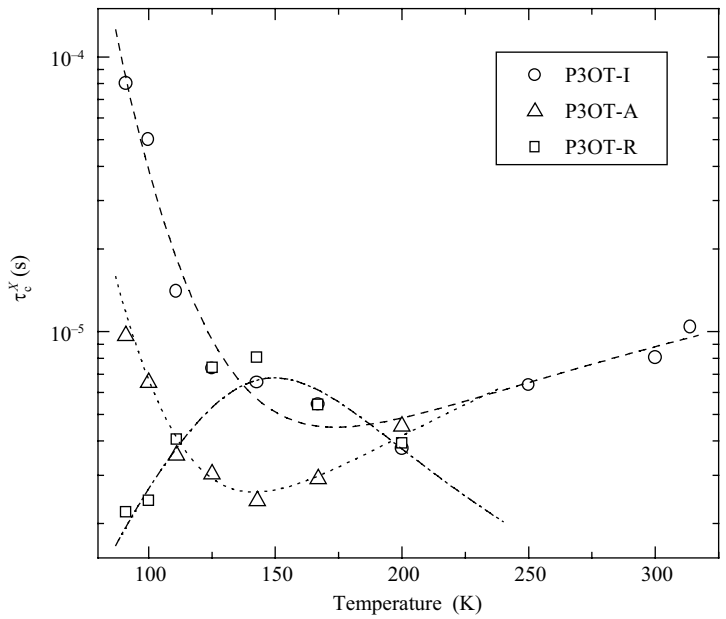

Fig. 8. Temperature dependence of the correlation time τ_c^X P3OT-I, P3OT-A and P3OT-R. The dependences calculated in framework of activation motion from Eq. (3) with $\tau_{c1}^0 = 1.3 \cdot 10^{-8}$ s, $E_a = 0.069$ eV, $k_1 = 3.1 \cdot 10^{-10}$ sK$^{-\beta}$, $\beta = 1.8$, $n = 1$ (dashed line), $\tau_{c1}^0 = 1.1 \cdot 10^{-8}$ s, $E_a = 0.054$ eV, $k_1 = 7.2 \cdot 10^{-12}$ sK$^{-\beta}$, $\beta = 2.5$, $n = 1$ (dotted line), $\tau_{c1}^0 = 6.3 \cdot 10^{-8}$ s, $E_a = 0.073$ eV, $k_1 = 3.1 \cdot 10^{-13}$ sK$^{-\beta}$, $\beta = 3.5$, $n = -1$ (dash-dotted line) are also shown.

$$\tau_c^X(T) = ((\tau_{c1}^0 \exp(E_a / k_B T))^n + (k_1 T^\beta)^n)^n . \quad (3)$$

Figure 8 shows that the dependences obtained experimentally for P3OT-I, P3OT-A, and P3OT-R are well fitted by Eq. (3) with $E_a = 0.069$ eV, $\beta = 1.8$, $n = 1$, $E_a = 0.054$ eV, $\beta = 2.5$, $n = 1$, and $E_a = 0.073$ eV, $\beta = 3.5$, $n = -1$ respectively. The activation energies obtained are close to those of macromolecular librations in other organic conducting polymers [36]. The preexponential factors are the lowest limit for the respective correlation times in these samples. The linear compressibility of an initial P3OT with planar chains is strongly anisotropic, being 2.5 times higher for the direction along the *a*-axis than along the *b*-axis [63]. It was proved that the low- and high-frequency modes exist in polythiophenes [64]. These modes differently superposed in P3OT above and below T_c should lead to the change of the n exponent in Eq. (3) from 1 for "successive" macromolecular dynamics in P3OT-I and P3OT-A to -1 for "parallel" molecular librations in P3OT-R. Osterbacka et al. [65] have found that the interchain coupling existing in self-assembled lamellae in P3AT drastically changes the properties of the polaron excitations and that the traditional self-localized polaron in one dimension is delocalized in two dimensions, resulting in a much reduced relaxation energy and multiple absorption bands.

The upper limit for the correlation time of anisotropic molecular motion in the systems under study registered by the ST-EPR method can be evaluated from equation [61]

$$\tau_c^X \leqslant \frac{2}{3\pi^2 T_1 \gamma_e^2 B_1^4} \frac{\sin^2\vartheta \cos^2\vartheta (B_\perp^2 - B_{||}^2)^2}{B_\perp^2 \sin^2\vartheta + B_{||}^2 \cos^2\vartheta}, \tag{4}$$

where γ_e is the gyromagnetic ratio, B_1 is the magnetic term of the microwave polarizing field, $B_\perp$ and $B_{||}$ are the anisotropic EPR spectrum components perpendicular and along the field, ϑ is the angle between an external magnetic field B_0 and the X-axis of the radical. The maximal correlation time was determined for P3OT-I sample from Eq. (4) to be $\tau_c^X = 4.4 \cdot 10^{-4}$ s at 66 K.

3.4 Dynamics of Polarons in P3OT

The spin-spin relaxation time of the P3OT samples determined from their X-band EPR absorption spectra as $T_2 = 2/\sqrt{3}\gamma_e \Delta B_{pp}$ and from their saturated D-band EPR dispersion spectra increases approximately by a factor of six. This means that the experimental data can rather be explained in terms of a modulation of spin relaxation by the polaron motion along the conjugated polymer chain segments with the diffusion coefficient $D_{1\text{-D}}$ and its hopping between the chains with the rate $D_{3\text{-D}}$. In the framework of such approach, the relaxation time of the electron or proton spins in the sample should vary depending on the spin precession frequency ω as $T_{1,2} \propto \sqrt{\omega}$ [66, 67] that should lead to the increase in relaxation times approximately by a factor of four. Note that the 2-D spin motion should lead to $T_{1,2} \propto \ln(\omega)$ dependence [66, 67] or to the increase of the relaxation times by factor of about two at the transition from X-band to D-band EPR.

Since the electronic relaxation is mainly determined by the dipole-dipole interaction between the spins, we can write the following equations for the rates of electronic relaxation [68]

$$T_1^{-1}(\omega_e) = \langle\omega^2\rangle[2J(\omega_e) + 8J(2\omega_e)], \tag{5}$$

$$T_1^{-1}(\omega_e) = \langle\omega^2\rangle[3J(0) + 5J(\omega_e) + 2J(2\omega_e)], \tag{6}$$

where $\langle\omega^2\rangle = 1/10(\mu_0/4\pi)^2\gamma_e^4\hbar^2 S(S+1)n\sum_{ij}$ is the averaged constant of the spin dipole interaction for a powderlike sample, μ_0 is the permeability for vacuum, $\hbar$ is the Planck constant, n is the number of polarons per monomer unit, $\sum_{ij}$ is the lattice sum for the powderlike sample, $J(\omega_e) = (2\Delta D_{1\text{-D}}\omega_e)^{-1/2}$ at $D_{1\text{-D}} \gg \omega_e \gg D_{3\text{-D}}$ or $J(\omega_e) = (2D_{1\text{-D}}D_{3\text{-D}})^{-1/2}$ at $D_{3\text{-D}} \gg \omega_e$ is the spectral density function for the 1-D motion, $D_{1\text{-D}} = 4D_{1\text{-D}}/L^2$, and L is the number of monomer units along which a spin is delocalized. The analogous spectral density function was used in the study of electron and proton spin dynamics in various conducting polymers [16, 36, 67].

In Fig. 9 are shown the temperature dependences of the effective dynamic parameters $D_{1\text{-D}}$ and $D_{3\text{-D}}$ calculated for PC in the initial and treated P3OT samples from the data presented in Fig. 7 with Eqs. (5) and (6) at $L \approx 5$ [69]. The

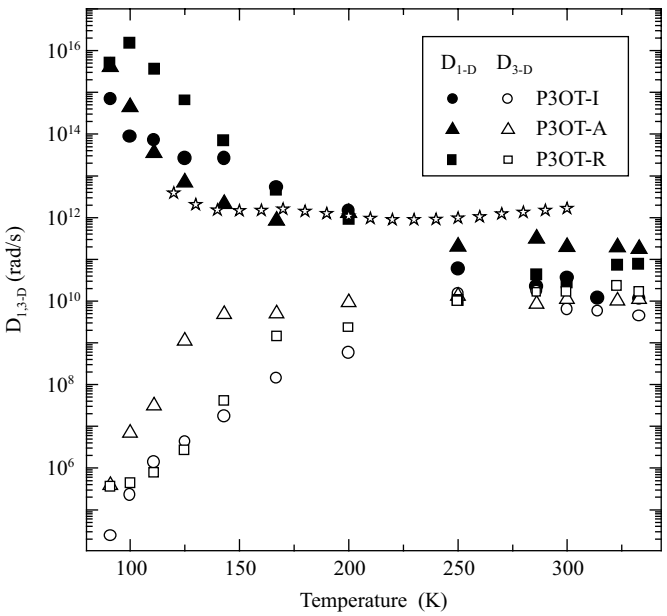

Fig. 9. Temperature dependences of the spin-charge diffusion coefficients along ($D_{1\text{-D}}$, filled symbols) and between ($D_{3\text{-D}}$, open symbols) polymer chains in the P3OT-I, P3OT-A and P3OT-R determined with Eqs. (5) and (6). Open stars show the $D_{1\text{-D}}(T)$ dependence calculated from Eq. (7) with ^{1}H NMR data for P3OT-I [31].

RT $D_{3\text{-D}}$ value obtained is about $D \approx 2.1 \cdot 10^{10}$ s^{-1} evaluated from the charge carrier mobility in slightly doped P3OT [29] and the $D_{1\text{-D}}$ value exceeds by 1–2 orders of magnitude the lower limit of the spin motion $v^0_{1\text{-D}}$. The RT anisotropy of spin dynamics $D_{1\text{-D}}/D_{3\text{-D}}$ increases from 6 in P3OT-I up to 18 in P3OT-A and decreases down to 2 in P3OT-R. At the temperature decreases down to 200 K this value increases up to 2500, 140, and 390 respectively, and then up to $3.8 \cdot 10^8$, $6.5 \cdot 10^7$, and $3.4 \cdot 10^{10}$, respectively, as the temperature decreases down to 100 K (Fig. 9).

In principle, the polaron 1-D diffusion coefficient $D_{1\text{-D}}$ can also be determined from the proton ^{1}H spin-lattice relaxation time $T_{1\text{p}}$ from [67]

$$T_{1\text{p}}^{-1}(\omega_\text{p},\omega_\text{e}) = \frac{1}{3}\left(\frac{\mu_0}{4\pi}\right)^2 \gamma_\text{e}^2\hbar^2 S(S+1)n\left[\frac{3}{5}d^2 J(\omega_\text{p}) + (a^2 + \frac{7}{5}d^2)J(\omega_\text{e})\right], \qquad (7)$$

where d and a are the dipolar and scalar electron-nuclear coupling constants respectively, ω_p is the proton angular precession frequency. The $D_{1\text{-D}}(T)$ dependence calculated from the ^{1}H 50 MHz spin-lattice relaxation data obtained by Masubuchi et al. [31] for P3OT-I with Eq. (7) is also presented in Fig. 9. It is seen from Fig. 9 that the $D_{1\text{-D}}$ value calculated from the NMR data is changed weaker with temperature. Besides, this value considerably exceeds the $D_{1\text{-D}}$ value obtained by

EPR at high temperatures and is close to that determined for the low-temperature region. Such discrepancy occurs probably because NMR is not a direct method for studying electron spin dynamics in this and other conducting polymers.

3.5 AC Conductivity of P3OT

The conductivity due to the 1-D and 3-D motion of N polarons each carrying an elemental charge e can be calculated from the equation

$$\sigma_{1,3\text{-D}} = Ne\mu_{1,3\text{-D}} = \frac{Ne^2 D_{1,3\text{-D}} d_{1,3\text{-D}}^2}{k_B T}, \tag{8}$$

where $\mu_{i\text{-D}}$ is the mobility of the polaron and $d_{i\text{-D}}$ are the lattice constants.

The temperature dependences of the conductivity due to polaron motion in the samples calculated from Eq. (8) with the lattice constants $d_{1\text{-D}} = c = 0.785$ nm and $d_{3\text{-D}} = b = 0.480$ nm [40] are shown in Fig. 10. It is seen that the anisotropy of conductivity $\sigma_{1\text{-D}}/\sigma_{3\text{-D}}$ depends on the system treatment. Indeed, this RT value increases from 15 in the P3OT-I up to 48 in the P3OT-A and decreases down to 4 in the P3OT-R (Fig. 10). The $\sigma_{1\text{-D}}/\sigma_{3\text{-D}}$ ratio depends also on the temperature of the samples increasing up to $6.8 \cdot 10^3$, $3.7 \cdot 10^2$, and $1.2 \cdot 10^3$ respectively, at $T = 200$ K and up to $1.0 \cdot 10^9$, $1.2 \cdot 10^8$, and $1.1 \cdot 10^{10}$ respectively at $T = 100$ K. This means that the charge dynamics as well as the spin and charge transfer mechanism depend on the structure and treatment of the polymer.

Analogously to the 1-D spin diffusion rate, the 1-D conductivity of the samples is characterized by the strong temperature dependence, $\sigma_{1\text{-D}}(T) \propto T^{-(7-9)}$ especially in the low-temperature region, when $T \leqslant T_c$ (Fig. 10). Note that the conductivity of organic salts frequently exhibits the $\sigma \propto T^{-2}$ relationship [54] and the $\sigma \propto T^{-1}$ dependence is typical for classical metals [70]. Such a behavior occurs also in other conducting polymers [36] and it is usually associated with the scattering of charge carriers on the optical lattice phonons. This model proposed for the charge transfer in conjugated polymers with metallike clusters [71, 72] predicts their intrinsic conductivity in the form

$$\sigma_{1\text{-D}}(T) = \frac{Ne^2 d_{1\text{-D}}^2 M t_0^2 k_B T}{8\pi\hbar\alpha^2}\left[\sinh\left(\frac{h\omega_{ph}}{k_B T}\right) - 1\right] = \sigma_0 T \cdot \left[\sinh\left(\frac{h\omega_{ph}}{k_B T}\right) - 1\right], \tag{9}$$

where M is the mass of the polymer unit, t_0 is the transfer integral equal for the π-electron approximately to 2.5–3 eV, ω_{ph} is the angular frequency of the optical phonon, and α is the constant of electron-phonon interaction equal for *trans*-PA to $\alpha = 4.1 \cdot 10^8$ eVcm^{-1} [72]. Note that the analogous metallike temperature behavior was also registered for intrachain polaron diffusion limited by macromolecular the librational scattering above T_c in undoped [73] and doped [38] polyanilines and poly(*bis*-alkylthioacetylene) [44].

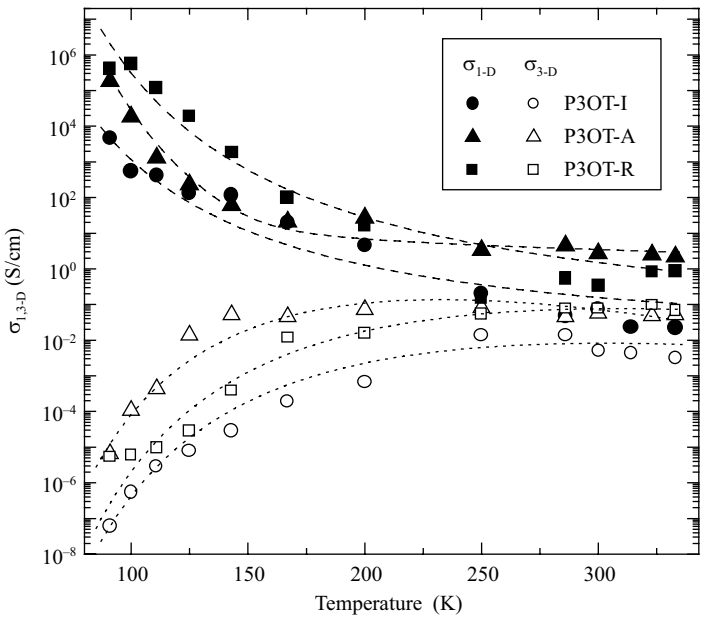

Fig. 10. Temperature dependences of the conductivity due to the spin-charge diffusion along ($\sigma_{1\text{-D}}$, filled symbols) and between ($\sigma_{3\text{-D}}$, open symbols) polymer chains in the P3OT-I, P3OT-A and P3OT-R. Dashed lines show the dependences calculated from Eq. (8) with $\sigma_0 = 7.1 \cdot 10^{-6}$ Scm^{-1}K^{-1} and $h\omega_{ph} = 0.13$ eV, $\sigma_0 = 5.5 \cdot 10^{-8}$ Scm^{-1}K^{-1} and $h\omega_{ph} = 0.20$ eV, $\sigma_0 = 1.1 \cdot 10^{-5}$ Scm^{-1}K^{-1} and $h\omega_{ph} = 0.18$ eV. The dependences calculated from Eq. (10) with $\sigma_0 = 9.1 \cdot 10^{-11}$ Ss$^{\gamma}$cm^{-1}K^{-1}, $\alpha = 2.1$, $E_a = 0.18$ eV (P3OT-I), $\sigma_0 = 3.1 \cdot 10^{-7}$ Ss$^{\gamma}$cm^{-1}K^{-1}, $\alpha = 3.6$, $E_a = 0.19$ eV (P3OT-A), and $\sigma_0 = 1.3 \cdot 10^{-9}$ Ss$^{\gamma}$cm^{-1}K^{-1}, $\alpha = 2.2$, $E_a = 0.19$ eV (P3OT-R) are shown by dotted lines.

Figure 10 shows that the intramolecular ac (140 GHz) conductivity calculated with Eq. (8) follows well Eq. (9) with the energy of optical phonons of 0.13 eV for P3OT-I, 0.20 eV for P3OT-A, and 0.18 eV for P3OT-R samples. This value is close to the energy of lattice phonons of 0.09–0.13 eV determined for doped polyanilines [37, 38] and 0.15–0.18 eV obtained for laser-modified poly(*bis*-alkylthioacetylene) [44].

The polaron-phonon interaction seems play an important role also in the interchain charge transfer at $T \geqslant T_c$. However, another mechanism should prevail at lower temperatures. Figure 10 shows that the interchain conductivity $\sigma_{3\text{-D}}$ increases with the temperature increase at the low-temperature region and then slightly decreases at $T \geqslant T_c$. The analogous dependence with the characteristic temperature $T_c \approx 150$ K was obtained for dc conductivity of P3HT [74] typical for the systems with a strong coupling of the charge with the lattice phonons. In this case the strong temperature dependence of the hopping conductivity is more evidently displayed in the ac conductivity. This interaction should lead to the narrow energy gap E_a much higher than the RT thermal energy ($k_B T \approx 0.026$ eV). The strong temperature dependence for σ_{ac} at low temperatures can be due to the thermal activation of the charge carriers from widely separated localized

states in the gap to closely localized states in the tails of the valence and conducting bands. In this case ac conductivity of P3OT can be written as [75]

$$\sigma_{3\text{-D}}(T) = \sigma_0 T \omega_e^{\gamma} \exp\left(-\frac{E_a}{k_B T}\right), \tag{10}$$

where $0 < \gamma < 1$ is a constant reflecting the dimensionality of the system and E_a is the activation energy of the charge carrier to extended states. Typical activation energies for the semiconducting, e.g., organic ion-radical salts are of the order of 0.1 eV [54]. The increase of the dimensionality of the polymer system should lead to the decrease in E_a. Parneix et al. [76] showed $\gamma = 1 - \alpha k_B T/E_a$ ($\alpha = 6$, $E_a = 1.1$ eV) dependence for poly(3-methylthiophene). So, we can use this approach for the explanation of the 3-D conductivity in the samples under study. Note that a nearly linear dependence of γ on E_a is characteristic for some other conducting polymers [77].

The temperature dependences calculated from Eq. (10) for the P3OT samples are shown in Fig. 10 as well. The activation energies obtained are close to the energy of lattice phonons of these samples determined above and also to that determined for the charge transfer in poly(tetrathiafulvalene) (0.2–0.3 eV) [78] and in laser modified poly(*bis*-alkylthioacetylene) (0.15–0.18 eV) [44].

DC conductivity of P3OT is close to 10^{-6} Scm^{-1} [27] and is mainly determined by the activation hopping of a charge carrier between high-conductive crystalline domains. Its intrinsic conductivity is defined by the $\sigma_{1\text{-D}}$ and $\sigma_{3\text{-D}}$ values, so the $\sigma_{1,3\text{-D}} \gg \sigma_{dc}$ relation should hold for all the samples.

4 Conclusion

Thus, the interaction of the spin charge carrier with the heteroatom in sulfurous organic polymer semiconductors P3OT leads to the appearance of the *g*-factor anisotropy in their D-band EPR spectra. Spin relaxation and dynamics are determined by the interaction of the mobile polaron with optical phonons of the polymer lattice. Polymer modification leads to a distinct change in magnetic, relaxation and dynamics properties of the polaron and its microenvironment. The correlations of the energies of the interchain spin diffusion, spin-spin interaction and the optical lattice phonons indicates the interaction of charge transport and molecular dynamics in these polymer semiconductors. These energies increase at the polymer treatment indicating the increase of its effective crystallinity. It can be concluded that the two types of charge transport mechanism can be associated with change in the lattice geometry at the characteristic (the polymer-glass transition) temperature T_c, e.g., with its thermochromic effect.

The relaxation, magnetic and dynamics properties of P3AT are expected to depend also on the alkyl group length and morphology of the sample. We plan to carry out an appropriate investigation also on P3HT and P3DDT to discuss these questions in the future publications.

The method provides the registration of fine structural, conformational and electron processes in various systems with their following interpretation in the frames of different theories. In high magnetic fields the interaction between spin packets in polymer decreases significantly, and they may be considered as non-interacting. This allows one to use the methods of steady-state saturation of spin packets and their saturation transfer to obtain more correct and complete information on spin relaxation and molecular dynamics in P3AT and other organic systems with lower dimensionality.

Acknowledgements

We thank N. N. Denisov, M. R. Zhdanov, and S. V. Tokarev for assistance in the EPR experiments. The work was supported by the German Ministry BMWI, Deutsche Forschungsgemeinschaft (DFG) Foundation, Grant 436 RUS 113/734/1-1 and by the Russian Foundation for Basic Research, Grants 01-03-33255 and 03-03-04005.

References

1. Kuzmany H., Mehring M., Roth S. (eds.): Elctronic Properties of Polymers. Berlin: Springer 1992.
2. Zerbi G.: Polyconjugated Materials. Amsterdam: North-Holland 1992.
3. Nalwa H.S. (ed.): Handbook of Organic Conductive Molecules and Polymers, vols. 1–4. New York: Willey 1997.
4. Scotheim T.E., Elsenbaumer R.L., Reynolds J.R. (eds.): Handbook of Conducting Polymers. New York: Marcel Dekker 1997.
5. Salaneck W.R., Clark D.T., Samuelsen E.J. (eds.): Science and Applications of Conducting Polymers. New York: Adam Hilger 1991.
6. Ashwell G.J. (ed.): Molecular Electronics. New York: Wiley 1992.
7. Chilton J.A., Gosey M.T. (eds.): Special Polymers for Electronic and Photonic Applications. London: Chapman and Hall 1995.
8. Kaeriyama K. in: Handbook of Organic Conductive Molecules and Polymers (Nalwa H.S., ed.), vol. 2, pp. 271–308. New York: Willey 1997.
9. Hotta S. in: Handbook of Organic Conductive Molecules and Polymers (Nalwa H.S., ed.), vol. 2, pp. 309–387. New York: Willey 1997.
10. Gronowitz S. (ed.): Thiophene and Its Derivatives. New York: Wiley 1991.
11. Inganas O., Salaneck W.R., Osterholm J.E., Laakso J.: Synth. Met. **22**, 395–398 (1988)
12. Inganas O. in: Handbook of Organic Conductive Molecules and Polymers (Nalwa H.S., ed.), vol. 3, pp. 785–793. New York: Willey 1997.
13. Kaniowski T., Niziol S., Sanetra J., Trznadel M., Pron A.: Synth. Met. **94**, 111–114 (1998)
14. Conwell E.M. in: Handbook of Organic Conductive Molecules and Polymers (Nalwa H.S., ed.), vol. 4, pp. 1–45. New York: Willey 1997.
15. Menon R. in: Handbook of Organic Conductive Molecules and Polymers (Nalwa H.S., ed.), vol. 4, pp. 47–145. New York: Willey 1997.
16. Mizoguchi K., Kuroda S. in: Handbook of Organic Conductive Molecules and Polymers (Nalwa H.S., ed.), vol. 3, pp. 251–317. New York: Willey 1997.
17. Carter F.L. (ed.): Molecular Electronic Devices, vols. 1 and 2. New York: Marcel Dekker 1982.
18. Bredas J.L., Chance R.R. (eds.): Conjugated Polymeric Materials: Opportunities in Electronics, Optoelectronics, and Molecular Electronics. Dordrecht: Kluwer Academic Publishers 1990.
19. Scrosati B. (ed.): Application of Electroactive Polymers. London: Chapman and Hall 1993.
20. Bobacka J., Ivaska A., Lewenstam A.: Anal. Chim. Acta **385**, 195–202 (1999)

21. Sariciftci N.S., Heeger A.J.: Synth. Met. **70**, 1349–1352 (1995)
22. Lee C.H., Yu G., Moses D., Pakbaz K., Zhang C., Sariciftci N.S., Heeger A.J., Wudl F.: Phys. Rev. B **48**, 15425–15433 (1993)
23. Lee K.H., Janssen R.A.J., Sariciftci N.S., Heeger A.J.: Phys. Rev. B **49**, 5781–5784 (1994)
24. Gebeyehu D., Padinger F., Fromherz T., Hummelen J.C., Sariciftci N.S.: Bull. Chem. Soc. Ethiopia **14**, 57–68 (2000)
25. Gebeyehu D., Brabec C.J., Padinger F., Fromherz T., Hummelen J.C., Badt D., Schindler H., Sariciftci N.S.: Synth. Met. **118**, 1–9 (2001)
26. Taka T., Jylha O., Root A., Silvasti E., Osterholm H.: Synth. Met. **55**, 414–419 (1993)
27. Chen T.A., Wu X.M., Rieke R.D.: J. Am. Chem. Soc. **117**, 233–244 (1995)
28. McCullough R.D., Lowe R.D., Jayaraman M., Ewbank P.C., Anderson D.L.: Synth. Met. **55**, 1198–1203 (1993)
29. Kunugi Y., Harima Y., Yamashita K., Ohta N., Ito S.: J. Mater. Chem. **10**, 2673–2677 (2000)
30. Heeger A.J., Kivelson S., Schrieffer J.R., Su W.P.: Rev. Mod. Phys. **60**, 781–850 (1988)
31. Masubuchi S., Imai R., Yamazaki K., Kazama S., Takada J., Matsuyama T.: Synth. Met. **101**, 594–595 (1999)
32. Lee S.B., Zakhidov A.A., Khairullin I.I., Sokolov V.Y., Khabibullaev P.K., Tada K., Yoshimoto K., Yoshino K.: Synth. Met. **77**, 155–159 (1996)
33. Marumoto K., Takeuchi N., Ozaki T., Kuroda S.: Synth. Met. **129**, 239–247 (2002)
34. Sensfuss S., Konkin A., Roth H.-K., Al-Ibrahim M., Zhokhavets U., Gobsch G., Krinichnyi V.I., Nazmutdinova G.A., Klemm E.: Synth. Met. **137**, 1433–1434 (2003)
35. Krinichnyi V.I.: 2-mm Wave Band EPR Spectroscopy of Condensed Systems. Boca Raton: CRC Press 1995.
36. Krinichnyi V.I.: Synth. Met. **108**, 173–222 (2000)
37. Krinichnyi V.I., Chemerisov S.D., Lebedev Y.S.: Phys. Rev. B **55**, 16233–16244 (1997)
38. Krinichnyi V.I., Roth H.-K., Hinrichsen G., Lux F., Lueders K.: Phys. Rev. B **65**, 155205-1-155205–14 (2002)
39. Roth H.-K., Krinichnyi V.I.: Synth. Met. **137**, 1431–1432 (2003)
40. Mardalen J., Samuelsen E.J., Gautun O.R., Carlsen P.H.: Synth. Met. **48**, 363–380 (1992)
41. Galkin A.A., Grinberg O.Y., Dubinskii A.A., Kabdin N.N., Krymov V.N., Kurochkin V.I., Lebedev Y.S., Oransky L.G., Shuvalov V.F.: Instrum. Eksp. Tekhn. **20**, 1229–1229 (1977)
42. Pelekh A.E., Krinichnyi V.I., Brezgunov A.Y., Tkachenko L.I., Kozub G.I.: Vysokomolekul. Soedin. A **33**, 1731–1738 (1991)
43. Iida M., Asaji T., Ikeda R., Inoue M.B., Inoue M., Nakamura D.: J. Mater. Chem. **2**, 357–360 (1992)
44. Krinichnyi V.I., Roth H.-K., Schroedner M.: Appl. Magn. Reson. **23**, 1–17 (2002)
45. Barta P., Niziol S., Leguennec P., Pron A.: Phys. Rev. B **50**, 3016–3024 (1994)
46. Cik G., Sersen F., Dlhan L., Szabo L., Bartus J.: Synth. Met. **75**, 43–48 (1995)
47. Kawai T., Mizobuchi H., Okazaki S., Araki H., Yoshino K.: Jap. J. Appl. Phys., Part 2 **35**, L640–L643 (1996)
48. Cik G., Sersen F., Dlhan L., Cerven I., Stasko A., Vegh D.: Synth. Met. **130**, 213–220 (2002)
49. Vonsovskii S.V.: Magnetism. Moscow: Nauka 1971.
50. Miller J.S., Epstein A.J.: Molecule-Based Magnets: An Introduction. Washington: American Chemical Society 1996.
51. Kahol P.K., Raghunathan A., McCormick B.J., Epstein A.J.: Synth. Met. **101**, 815–816 (1999)
52. Krinichnyi V.I., Herrmann R., Fanghaenel E., Moerke W., Lueders K.: Appl. Magn. Reson. **12**, 317–327 (1997)
53. Geschwind S. (ed.): Electron Paramagnetic Resonance. New York: Plenum Press 1972.
54. Williams J.M., Ferraro J.R., Thorn R.J., Carlson K.D., Geiser U., Wang H.H., Kini A.M., Whangboo M.-H.: Organic Superconductors (Including Fullerenes): Synthesis, Structure, Properties, and Theory. Englewood Cliffs, N.J.: Prentice-Hall 1992.
55. Cameron T.S., Haddon R.C., Mattar S.M., Parsons S., Passmore J., Ramirez A.P.: J. Chem. Soc. Chem. Commun. **1991**, 358–360.
56. Cameron T.S., Haddon R.C., Mattar S.M., Parsons S., Passmore J., Ramirez A.P.: J. Chem. Soc. Dalton Trans. **1992**, 1563–1572.
57. Bock H., Rittmeyer P., Krebs A., Schultz K., Voss J., Kopke B.: Phosph. Sulf. Silic. Relat. Elem. **19**, 131–134 (1984)

58. Owens J.: Phys. Status Solidi B **79**, 623–626 (1977)
59. Elliott R.J.: Phys. Rev. **96**, 266–279 (1954)
60. Gullis P.R.: J. Magn. Reson. **21**, 397–404 (1976)
61. Hyde J.S., Dalton L.R. in: Spin Labeling. Theory and Application (Berliner L.J., ed.), vol. 2, chapt. 1. New York: Academic Press 1979.
62. Krinichnyi V.I., Grinberg O.Y., Dubinskii A.A., Livshits V.A., Bobrov Yu.A., Lebedev Y.S.: Biofizika **32**, 534–535 (1987)
63. Mardalen J., Samuelsen E.J., Konestabo O.R., Hanfland M., Lorenzen M.: J. Phys. Condens. Matter **10**, 7145–7154 (1998)
64. Sauvajol J.L., Bormann D., Palpacuer M., LerePorte J.P., Moreau J.J.E., Dianoux A.J.: Synth. Met. **84**, 569–570 (1997)
65. Osterbacka R., An C.P., Jiang X.M., Vardeny Z.V.: Synth. Met. **116**, 317–320 (2001)
66. Butler M.A., Walker L.R., Soos Z.G.: J. Chem. Phys. **64**, 3592–3601 (1976)
67. Nechtschein M. in: Handbook of Conducting Polymers (Skotheim T.A., Elsenbaumer R.L., Reynolds J.R., eds.), pp. 141–163. New York: Marcel Dekker 1997.
68. Abragam A.: The Principles of Nuclear Magnetism. Oxford: Clarendon Press 1961.
69. Devreux F., Genoud F., Nechtschein M., Villeret B. in: Electronic Properties of Conjugated Polymers (Kuzmany H., Mehring M., Roth S., eds.), Springer Series in Solid State Sciences, vol. 76, pp. 270–276. Berlin: Springer 1987.
70. Blakemore G.S.: Solid State Physics. Cambridge: Cambridge University Press 1985.
71. Pietronero L.: Synth. Met. **8**, 225–231 (1983)
72. Kivelson S., Heeger A.J.: Synth. Met. **22**, 371–384 (1988)
73. Pratt F.L., Blundell S.J., Hayes W., Nagamine K., Ishida K., Monkman A.P.: Phys. Rev. Lett. **79**, 2855–2858 (1997)
74. Yamauchi T., Najib H.M., Liu Y.W., Shimomura M., Miyauchi S.: Synth. Met. **84**, 581–582 (1997)
75. Mott N.F., Davis E.A.: Electronic Processes in Non-Crystalline Materials. Oxford: Clarendon Press 1979.
76. Parneix J.P., El Kadiri M. in: Electronic Properties of Conjugated Polymers (Kuzmany H., Mehring M., Roth S., eds.), Springer Series in Solid State Sciences, vol. 76, pp. 23–26. Berlin: Springer, 1987.
77. El Kadiri M., Parneix J.P. in: Electronic Properties of Polymers and Related Compounds (Kuzmany H., Mehring M., Roth S., eds.), Springer Series in Solid State Sciences, vol. 63, pp. 183–187. Berlin: Springer 1985.
78. Gruber H., Roth H.-K., Patzsch J., Fanghaenel E.: Makromolekulare Chemie-Macromolecular Symposia **37**, 99–113 (1990)

Authors' address: Vector I. Krinichnyi, Institute of Problems of Chemical Physics, Chernogolovka, Moscow Region, 142432, Russian Federation
E-mail: kivi@cat.icp.ac.ru